Analytical Methods

Dynamic Article Links

Cite this: *Anal. Methods*, 2011, **3**, 1494

www.rsc.org/methods

PAPER

Spectrofluorimetric study of the herbicide bentazone in organized media: analytical applications

Javier A. Porini and Graciela M. Escandar*

Received 18th January 2011, Accepted 11th May 2011
DOI: 10.1039/c1ay05028a

The present work is devoted to the study of the spectrofluorimetric behavior of the herbicide bentazone in the presence of selected organized assemblies, with the purpose of optimizing the working conditions for its determination in environmental samples. Bentazone is one of the most applied herbicides in countries of profuse agriculture, and belongs to the group of relevant persistent pollutants. Among the studied media, methyl-β-cyclodextrin produced the largest fluorescence signals for bentazone, and was selected as auxiliary reagent for the quantitative analyses. The selectivity of the method, *i.e.*, its capability to measure accurately an analyte in the presence of interferents that may be present in the sample matrix, was improved through second-order multivariate calibration, measuring excitation–emission fluorescence matrices for both artificial and real samples, and processing them with the algorithm parallel-factor analysis (PARAFAC). A detection limit of 3 ng mL^{-1} and a relative error of prediction of 5.6% for bentazone were obtained in samples without interferents. In samples containing seven additional agrochemicals acting as interferences, the limit of detection and the relative error of prediction were 5 ng mL^{-1} and 9.9%, respectively. The method was successfully applied to spiked natural water samples, with statistical parameters in these cases which were similar to those calculated in samples with interferences. In this study, the advantages of coupling fluorescence measurements in organized media and second-order chemometric analysis are exploited in order to rapidly quantify a frequent pollutant at low concentrations in a very interfering medium and using green chemicals.

Introduction

Effluent irrigation is a current practice in agriculture due to its known beneficial effects such as provision of nutrients for plant growth and improvement of soil structure. However, effluents may contain anthropogenic contaminants (heavy metals, pharmaceuticals, pesticides, *etc.*), which are dispersed in the environment through this procedure, producing adverse effects in people and animals directly or indirectly exposed.[1] Therefore, monitoring the potential presence of these environmental contaminants is essential to prevent their serious consequences.

Molecular luminescence techniques are extensively applied for determining compounds of environmental risk due to their inherent advantages of sensitivity and selectivity.[2] The sensitivity of these methods can be even further enhanced by the use of organized media. The latter is a term used to describe different systems such as cyclodextrin (CD) and micelles, which can compartmentalize organic compounds, sequestering them from the bulk environment, and improving in this way their photoluminescence properties.

With the purpose of developing a new spectrofluorimetric method for the determination of the herbicide bentazone (BTZ, 3-isopropyl-1H-2,1,3-benzothiadiazin-4(3H)-one-2,2-dioxide, Fig. 1), the effect of different organized assemblies in its fluorescence signal was analyzed. BTZ is a widely used herbicide for post-emergence control of sedges and broadleaf weeds in winter and spring cereals.[3] In a recent ground water monitoring study for polar organic persistent pollutants in European countries,[4] BTZ showed to be one of the most relevant chemicals found, with a frequency of detection of 32% and a maximum concentration of 11 ng mL^{-1}. On the other hand, BTZ ranks third of the major pesticides causing problems in drinking water supply from bank filtration in Germany.[5] Peschka *et al.*[6] reported that BTZ represents one of the most applied herbicides in the Ebro river delta (Spain), which holds a network of irrigation and drainage channels, where the concentration of BTZ reaches a mean concentration of 31 ng mL^{-1} during the application time from May to August.

BTZ displays fluorescence in several organic solvents,[7,8] and these signals were used for either its direct determination[7] or for

Instituto de Química Rosario (CONICET-UNR), Facultad de Ciencias Bioquímicas y Farmacéuticas, Universidad Nacional de Rosario, Suipacha 531, 2000 Rosario, Argentina. E-mail: escandar@iquir-conicet.gov.ar

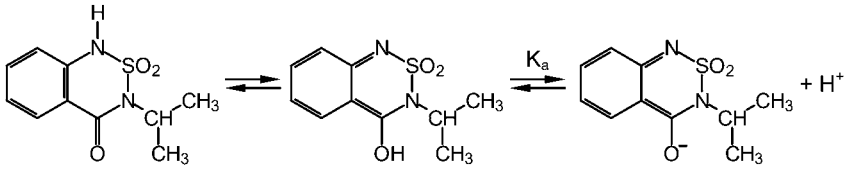

Fig. 1 Bentazone (BTZ): keto–enol tautomerism and deprotonation equilibrium.

its detection after chromatographic analysis.[9–11] However, the native fluorescence of BTZ in water is weak, and only a solid-phase spectrofluorimetric method has been reported, using an anion-exchange gel for BTZ quantitation in aqueous solution.[12]

In the present paper, the spectrofluorimetric behavior of BTZ in the presence of eight native and modified cyclodextrins and six different micellar media is studied, and thus the optimal analytical working conditions are established. Very recently, complexation of BTZ with β-CD and sulfobutylether-β-CD has been studied by differential pulse voltammetry.[13]

Since real matrices may contain other compounds which could interfere in the spectrofluorimetric determination of BTZ, a second-order multivariate method is proposed for its quantitative analysis. Specifically, the algorithm parallel factor analysis (PARAFAC)[14] was applied to excitation–emission fluorescence matrices (EEFMs) of BTZ under optimal working conditions and in the presence of other fluorescent agrochemicals acting as potential interferents. This usually employed algorithm has the advantage of allowing concentration and spectral profiles of the analyte under study to be extracted in the presence of any number of unexpected constituents ('second-order advantage').[15]

The feasibility of determining BTZ in real matrices is demonstrated by applying the proposed methodology to river and stream water samples.

Experimental

Reagents and solutions

All reagents were of high-purity grade and used as received. Bentazone and carbendazim (CBZ) were obtained from Riedel-de Haën (Seelze, Germany). Methyl-β-cyclodextrin (M-β-CD), sulfate-β-cyclodextrin sodium salt (S-β-CD), heptakis(2,6-di-O-methyl)-β-cyclodextrin (DM-β-CD), hexadecyltrimethylammonium bromide (HTAB), 1-naphthaleneacetic acid (NAA), dichlorophene (DCP), carbaryl (CBL) and thiabendazole (TBZ) were purchased from Sigma-Aldrich (Milwaukee, WI, USA). Hexadecyltrimethylammonium chloride (HTAC), decyltrimethylammonium bromide (DeTAB), (2-hydroxyethyl)-β-cyclodextrin (HE-β-CD), Brij 35, fuberidazole (FBZ) and carbofuran (CBF) were provided by Fluka (Buchs, Switzerland). Sodium dodecylsulfate (SDS), Triton X100, and methanol were obtained from Merck (Darmstadt, Germany). α-, β- and γ-cyclodextrins (α-CD, β-CD and γ-CD), and (2-hydroxypropyl)-β-cyclodextrin (HP-β-CD) were acquired from Cyclolab (Budapest, Hungary).

Methanol stock solutions of BTZ, CBL, FBZ, TBZ, NAA, CBF, DCP and MBC (*ca.* 1000 μg mL^{-1}) were prepared and stored in dark flasks at 4 °C. From these solutions, working aqueous solutions were prepared by taking appropriate aliquots, evaporating the organic solvent by use of dry nitrogen and diluting with ultrapurified water, from a Millipore system (Massachusetts, USA) to the desired concentrations. Stock solutions of CDs and surfactants were prepared in ultrapurified water.

Apparatus

Fluorescence measurements were done on an Aminco Bowman (Rochester, NY, USA) Series 2 luminescence spectrometer equipped with a 150 W xenon lamp and using 1.00 cm quartz cell, slit widths of 4 nm, exciting at 330 nm and obtaining the fluorescence emission at 436 nm. EEFMs were collected using the wavelength excitation range of 240–372 nm (each 4 nm) and the wavelength emission range of 390–470 nm (each 1 nm). Absorbance data were obtained with a Beckman (Fullerton, CA, USA) DU 640 spectrophotometer. The temperature of the cell holder was regulated using a Lauda (Frankfurt, Germany) RM6T thermostatic bath. The pH of solutions was measured with a Metrohm (Herisau, Switzerland) 713 pHmeter equipped with glass and Ag/AgCl reference electrodes.

Influence of cyclodextrin and surfactant concentrations

For all systems (except for β-CD) the following procedure was performed: 2.00 mL of 500 ng mL^{-1} BTZ were spiked with increasing volumes of each CD or surfactant solutions also containing 500 ng mL^{-1} BTZ, in order to avoid analyte dilution. After each addition, the fluorescence spectrum was read. With the purpose of obtaining the blank signals, a similar procedure was also performed in the absence of BTZ. Finally, blank signals were subtracted from the corresponding spectra and the plot of the corrected fluorescence intensity at a maximum as a function of either CD or surfactant concentration was obtained.

Because of the relatively low aqueous solubility of β-CD (~0.01 mol L^{-1}), the latter procedure cannot be applied since a concentrated CD solution would be required as titrating agent. Therefore, in this case the experiment was divided in two steps. In the first step, increasing aliquots of 0.01 mol L^{-1} β-CD were added to a BTZ solution contained in the cell until a final CD concentration was about 0.005 mol L^{-1}. It is necessary to point out that the titrating β-CD solution also contained BTZ in order to avoid dilution of the analyte. In a second step, to a solution containing BTZ and 0.01 mol L^{-1} β-CD, increasing aliquots of BTZ solution (in order to avoid BTZ dilution) were added up to a final β-CD concentration in the cell of about 0.005 mol L^{-1}. Similar procedures, but in the absence of BTZ, were carried out for the blanks. Finally, the corrected intensity fluorescence measured in each experimental point of both experiments was plotted as a function of the β-CD concentration, and a complete curve in the β-CD range 0–0.01 mol L^{-1} was obtained.

Influence of the pH

To a stirred hydrochloric acid solution (pH ≈ 2) of 500 ng mL^{-1} BTZ (in the presence or absence of selected organized media at the corresponding optimal concentration), NaOH solution (0.05–1 mol L^{-1}, as appropriate) was added in small increments. For each pH point, the solution was aliquoted (2 mL), the emission spectrum was read, and the extracted volume was then restored to the vessel. This procedure was repeated until pH ≈ 9–10 was achieved.

Chemometric analysis coupled to EEFMs

The theory of PARAFAC is well documented and a brief description can be found in previous reports.[16,17]

For the quantitative analysis, all solutions were prepared in the presence of 0.02 mol L^{-1} M-β-CD. Since the goal of the present work was to detect low levels of BTZ, the maximum assayed concentration of BTZ was about 300 ng mL^{-1}, and no attempts were made to establish the upper concentration of the linear range.

Sets of five calibration samples, fifteen validation samples and twenty test samples were prepared at different concentrations of BTZ following a random design in the concentration range indicated above. Validation samples serve to test the predictive ability of the model in the absence of interferents. On the other hand, test samples are used for the same purpose but in the presence of unexpected compounds. Therefore, test samples did also contain high levels of seven foreign agrochemicals acting as interferents. The maximum concentrations of CBL, FBZ, TBZ, NAA, CBF, DCP and MBC in these latter samples were 4200; 3000; 4350; 5000, 5000; 4500 and 5000 ng mL^{-1}, respectively.

For a recovery analysis in real environmental matrices, a river water sample (Paraná River, Argentina) was collected near a region of high industrial activity, and stream water samples (Ludueña stream, Argentina) were obtained from two regions located at about 10 km away from each other and near sewage discharges, containing significant amounts of fluorescent humic acids and proteic substances. Because these samples did not contain BTZ at the level detected by the proposed method, they were first spiked with the analyte and then filtered through a filter paper to remove suspended sediments and solid materials.

Results and discussion

Spectral characteristics of BTZ

The UV spectrum of BTZ in aqueous solution shows an intense absorption at 223 nm and wide bands with maxima located at 250 (shoulder), 274, 283 (shoulder) and 330 nm (Fig. 2A). Besides, Fig. 2B shows the excitation fluorescence spectrum of BTZ in aqueous solution at neutral pH, with maxima at about 250 and 330 nm, and a wide emission spectrum with a maximum at about 430 nm. Consequently, for zeroth-order experiments, 330 and 430 nm were selected as excitation and emission wavelengths, respectively.

BTZ is a weak acid with pK_a = 3.28,[5] therefore, below pH 3 it is present in its tautomeric neutral forms (Fig. 1), and above this pH value, BTZ suffers deprotonation to its anionic structure. With the purpose of studying the behavior of the BTZ fluorescence intensity with the pH, and thus to optimize this latter parameter, an acid–base titration experiment was performed. As can be seen in Fig. 3, the fluorescence intensity of BTZ reaches its maximum and remains almost constant in the pH range 4–9, where BTZ is in its anionic form, suggesting that this broad pH region is optimal for fluorescence experiments. Further, the inflection of this profile at about pH 3.5 suggests that the acidity behavior of BTZ in its excited state is similar to that in the ground state, indicating that the fluorescence decay process is faster than the deprotonation in the excited state.[18]

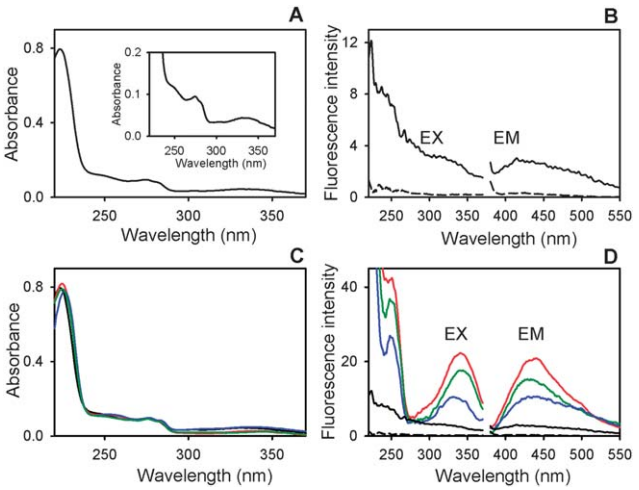

Fig. 2 (A) Absorption spectrum of an aqueous solution of 2000 ng mL^{-1} BTZ. (B) Excitation (EX) and emission (EM) fluorescence spectra of an aqueous solution of 160 ng mL^{-1} BTZ. (C) Background-corrected spectra of 2000 ng mL^{-1} BTZ in the presence of 0.018 mol L^{-1} M-β-CD (red line), 0.037 mol L^{-1} DM-β-CD (green line) and 0.018 mol L^{-1} HTAB (blue line). (D) Background-corrected EX–EM fluorescence spectra of 160 ng mL^{-1} BTZ in the presence of 0.015 mol L^{-1} M-β-CD (red line), 0.015 mol L^{-1} DM-β-CD (green line) and 0.015 mol L^{-1} HTAB (blue line). Photomultiplier tube (PMT) = 700 V.

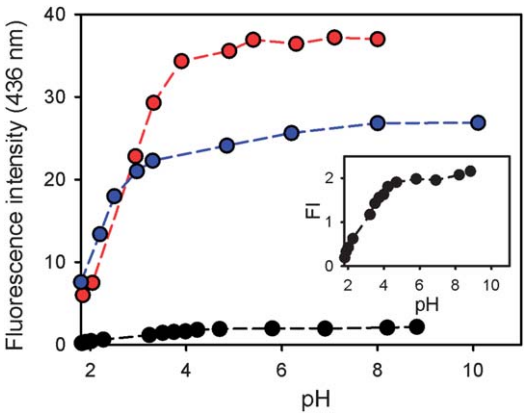

Fig. 3 Experimental fluorescence values *vs.* pH for BTZ (black circles), BTZ–M-β-CD (red circles) and BTZ–HTAB (blue circles) solutions. C_{BTZ} = 530 ng mL^{-1}, $C_{M\text{-}\beta\text{-}CD}$ = 0.020 mol L^{-1}, C_{HTAB} = 0.020 mol L^{-1}.

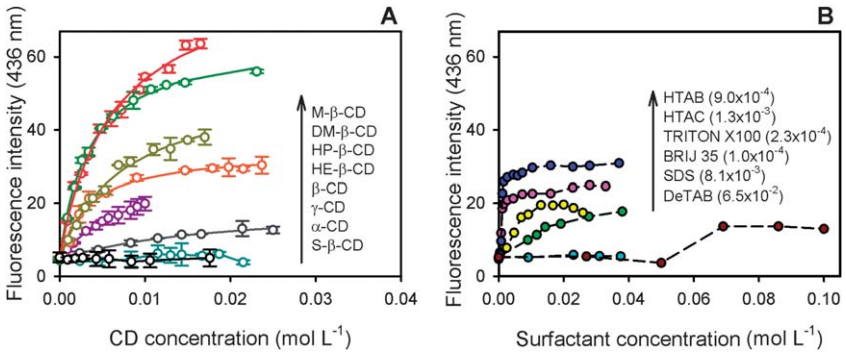

Fig. 4 (A) Effect of cyclodextrins in the fluorescence emission of BTZ. S-β-CD (black), α-CD (dark cyan), γ-CD (gray), β-CD (violet), HE-β-CD (orange), HP-β-CD (dark yellow), DM-β-CD (dark green) and M-β-CD (red). (B) Effect of surfactants in the fluorescence emission of BTZ. DeTAB (dark red), SDS (light blue), Brij 35 (green), Triton X100 (yellow), HTAC (pink) and HTAB (blue). The corresponding CMC in mol L^{-1} are indicated within parenthesis (ref. 19). $C_{BTZ} = 530$ ng mL^{-1}, $\lambda_{ex} = 330$ nm; PMT = 700 V. For comparison, the vertical axes are shown in the same scale. Each point was corrected with the corresponding background.

Cyclodextrins influence

The three major cyclodextrins, α-, β-, and γ-CDs, which comprise six, seven, and eight glucose units, respectively, and the β-CD derivatives M-β-, HE-β-, HP-β-, S-β- and DM-β-CDs were investigated. In Fig. 4A, the intensities of the fluorescence emissions of BTZ at different concentrations of the evaluated CDs are displayed.

As can be seen, among the three native CDs, α-CD does not appreciably modify the fluorescence properties of BTZ, a slight increase of fluorescence is verified in the presence of γ-CD, and the β-CD cavity appears to be the best medium for our purposes. It is possible that the cavity sizes of α- (smaller than β-CD) and γ-CD (larger than β-CD) are not appropriate for an optimal protective effect towards non-radiative decay processes occurring in the bulk solution.

It is also possible that substituents present in the β-CD structure are able to produce either a positive or negative effect in the host–guest interaction leading to an increase in fluorescence. This implies that the polarity of the host contributes to the complex formation in addition to the cavity size. For example, the sulfate groups in S-β-CD produces electrostatic repulsion, a poor interaction between the anionic analyte and this negatively charged CD is verified, and no significant changes in fluorescence intensity are observed (see Fig. 4A). Other less polar substituents such as 2-hydroxyethyl, 2-hydroxypropyl, methyl, and heptakis(2,6-di-O-methyl) possess a favorable effect toward the complex formation and therefore on the corresponding intensity enhancement.

From the profiles shown in Fig. 4A, the 1 : 1 association constants of BTZ with γ-, β-, HE-β-, HP-β-, DM-β- and M-β-CDs were determined by applying non-linear regression analysis, and the obtained results are shown in Table 1. These values denote a moderate interaction with the evaluated CDs (K values in the order of 100–300 L mol^{-1}), which is not necessarily related to the intensity of the maximum luminescence signal obtained. Thus, although the largest inclusion constant corresponds to the BTZ–DM-β-CD complex, higher fluorescence intensity is achieved with M-β-CD at concentrations higher than 0.015 mol L^{-1} (Fig. 4A).

It is interesting to note that the presence of either M-β-CD or DM-β-CD does not produce significant changes in the UV spectrum of BTZ (Fig. 2C). However, the fluorescence intensity of BTZ in the presence of both CDs is drastically enhanced, especially in the case of M-β-CD (Fig. 2D) where this intensity is increased about eight fold. Therefore, this latter CD was selected for the subsequent quantification experiments.

In order to study the changes in the fluorescence intensity of BTZ as a function of pH in the presence of M-β-CD, the acid–base fluorimetric titration was performed in the presence of a constant concentration of this CD (Fig. 3). A similar acid–base behavior is observed in comparison with the system without CD, with lower signal intensities at pH below 3 than those obtained at pH larger than 4. This result suggests that the keto–enol group, which suffers the deprotonation process, remains outside the CD cavity while the non-polar benzene ring would be included in the CD cavity.

Table 1 Inclusion constants for BTZ–CD complexes at 20 °C

CDs	K^a/L mol^{-1}	Literature value[b]
γ-CD	59 (10)	
β-CD	105 (8)	118 (20), ref. 13
HE-β-CD	287 (40)	
HP-β-CD	134 (14)	
DM-β-CD	293 (13)	
M-β-CD	160 (14)	

[a] Standard deviation from duplicates between parentheses. [b] Calculated by differential pulse voltammetry. Standard deviation from triplicates between parentheses.

Micellar-enhanced fluorescence

The influence of micelles on the fluorescence intensity of BTZ was also studied. This was done by keeping a constant concentration of the herbicide, and increasing the concentrations of each surfactant (Fig. 4B). In order to ensure the micelle formation, the maximum concentrations of the evaluated surfactants were higher than the corresponding critical micelle concentrations.[19]

With the exception of SDS, all studied micellar systems produced signal enhancements of different degrees. The negative sulfonyl group in the SDS molecule would avoid the interaction with the negatively charged molecule of BTZ at neutral pH. An opposite effect is corroborated in the case of the cationic surfactants (DeTAB, HTAB and HTAC), where fluorescence increments of different magnitudes were verified. In these cases, the length of the non-polar chain of the surfactant involved in the micelle formation seemed to be important in the protection of the lowest excited state of BTZ from non-radiative processes, since the signals obtained in the presence of DeTAB are significantly less intense than those provided by HTAB and HTAC micellar systems. Finally, neutral surfactants (Brij 35 and Triton X100) produced a moderate fluorescence enhancement at concentrations of about 0.02 mol L^{-1}.

In conclusion, among the studied surfactants, HTAB showed to be the best one in terms of fluorescence enhancement (Fig. 4B), although the maximum intensity reached was lower than that obtained with the several studied CDs (Fig. 2D).

As in the CD systems, it was also corroborated that the presence of surfactants did not produce significant changes in the absorbance spectrum of BTZ (Fig. 2C).

The profile of fluorescence intensity as a function of pH in the BTZ–HTAB system (Fig. 3) showed an inflection near pH 2.3, suggesting that the presence of the cationic surfactant promotes the deprotonation of the enol group of BTZ with the concomitant ion pair formation between the anionic BTZ structure and the cationic surfactant.

Effect of temperature

The influence of the temperature on the fluorescence emission of BTZ in the presence of either M-β-CD or HTAB was evaluated. In both systems, the experiments showed that a temperature decrease only leads to a slight fluorescence intensity improvement. For example, if the experiment is conducted at 10 °C, the fluorescence increases by less than 20% of the original value at 20 °C. Therefore, no efforts were made to keep a low working temperature, and the quantitative analysis was performed at 20 °C.

Quantitative analyses

On the basis of the experiments described above, the optimal experimental conditions for the determination of BTZ by spectrofluorimetry can be established (Table 2). In the case of quantifying the herbicide in simple matrices and in the absence of interferents, a direct zeroth-order calibration could be carried out. However, taking into account that environmental samples can contain interferent compounds, a second-order chemometric analysis was proposed by using PARAFAC, a popular and easy to implement algorithm which achieves the second-order advantage.

Initially, EEFMs were recorded for calibration and validation samples under the working conditions indicated in Table 2. Fig. 5A shows the contour plot corresponding to the tridimensional EEFM for a typical validation sample in the analyzed wavelength ranges. PARAFAC was applied to three-way data arrays built by joining the data matrices for each of the validation samples in turn, with those for the set of calibration samples. The algorithm was initialized with the loadings giving the best fit after a small number of trial runs, selected from the comparison of the results provided by generalized rank annihilation[20] and several orthogonal random loadings. The number of components was selected applying three procedures: (1) taking into account the results of the so-called core consistency analysis,[21] (2) through the analysis of PARAFAC residuals,[14] and (3) considering that the addition of subsequent components did not generate repeated profiles. The results obtained by the three procedures were consistent and established that the number of total components required by PARAFAC in validation samples was two, corresponding to the analyte and to a background signal.

Table 2 Instrumental and chemical parameters for the chemometric analysis

	Values
Selected excitation range/nm	240–372
Selected emission range/nm	390–470
Slits (excitation/emission)/nm	4/4
Photomultiplier voltage/V	700
Calibration range/ng mL^{-1}	0–300
$C_{M\text{-}\beta\text{-}CD}$/mol L^{-1}	0.02
pH	~7
Temperature/°C	20

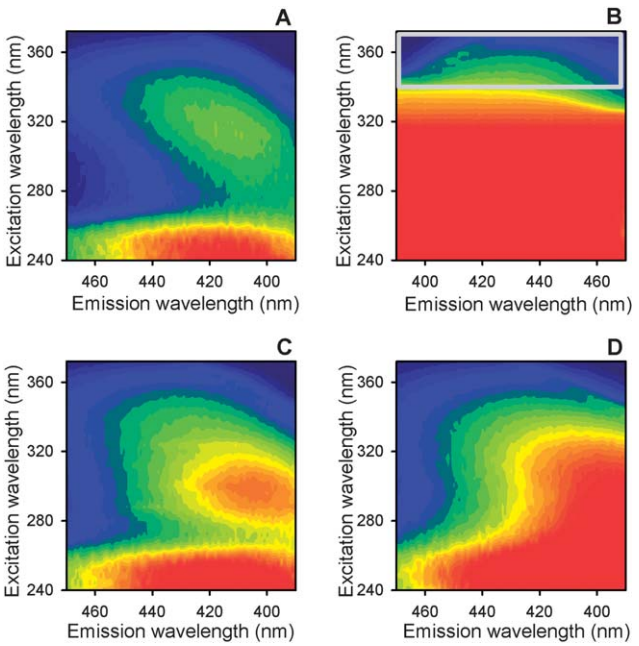

Fig. 5 Two-dimensional contour plots of the EEFMs corresponding to (A) a validation sample containing 154 ng mL^{-1} BTZ, (B) a test sample containing 154 ng mL^{-1} BTZ, and 2700 ng mL^{-1} CBL, 1950 ng mL^{-1} FBZ, 4350 ng mL^{-1} TBZ, 3600 ng mL^{-1} NAA, 4800 ng mL^{-1} CBF, 4100 ng mL^{-1} DCP and 5000 ng mL^{-1} MBC, (C) a river sample added with 100 ng mL^{-1} BTZ, and (D) a stream sample added with 150 ng mL^{-1} BTZ. The gray line in (B) indicates the selected wavelength region for PARAFAC processing.

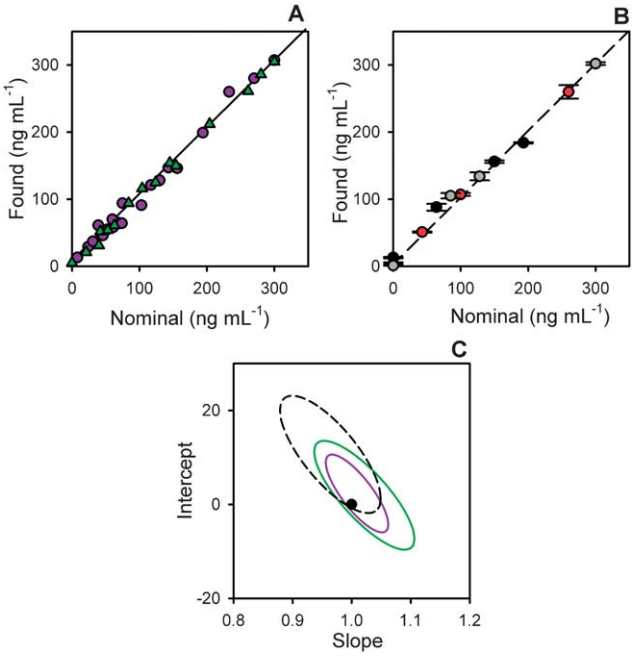

Fig. 6 Plots of BTZ predicted concentrations as a function of the nominal values using PARAFAC in validation samples (green triangles) and in artificial samples with interferents (violet circles) (A); and in a river sample (red circles) and two different stream samples (black and gray circles) spiked with the analyte (error bars correspond to duplicates) (B). Elliptical joint regions (at 95% confidence level) for the slopes and intercepts of the regressions for validation samples (green line), artificial (violet line) and real samples (black dashed line) predictions (C). The black circle in the elliptical plots marks the theoretical (intercept = 0, slope = 1) point.

Table 3 Statistical results for BTZ using the proposed method

	Validation samples[a]	Test samples[b]	Real water samples[c]
RMSEP[d]/ng mL^{-1}	7	11	11
REP[e] (%)	5.6	9.9	9.9
LOD[f]/ng mL^{-1}	3	5	5
LOQ[g]/ng mL^{-1}	9	15	15

[a] Fifteen samples. [b] Twenty samples containing CBL, FBZ, TBZ, NAA, CBF, DCP and MBC as interferents. [c] Three different natural waters evaluated at four BTZ levels each (sixteen samples, see text). [d] RMSEP, root-mean-square error of prediction. [e] REP, relative error of prediction. [f] LOD, limit of detection calculated according to ref. 26. [g] LOQ, limit of quantitation calculated as LOD × (10/3.3).

Fig. 6 shows the predicted values in comparison with the nominal ones. Both the elliptical joint confidence region (EJCR, ref. 22) test for the slope and intercept of the above plot and the corresponding statistical results (Table 3) suggest a high-quality prediction.

Because the real challenge in the routine laboratory is to obtain satisfactory predictions in systems where other foreign compounds are also present, seven fluorescent agrochemicals which overlap their spectra in different degrees with those of BTZ were introduced in test samples for evaluation. The selected

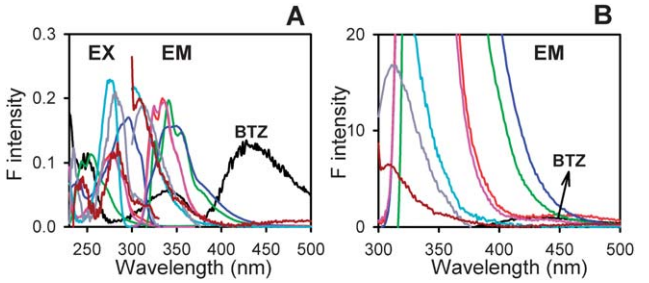

Fig. 7 (A) Normalized excitation (EX) and emission (EM) fluorescence spectra for BTZ (black), CBL (red), FBZ (green), TBZ (blue), NAA (pink), CBF (light blue), DCP (gray) and MBC (dark red) in aqueous solution. (B) Emission (EM) fluorescence spectra of BTZ and agrochemicals at typical concentrations used in the test samples. The λ_{ex} (nm)/λ_{em} (nm) are: 330/436, 275/333, 292/340, 295/350, 278/330, 278/306, 285/336 and 295/340 for BTZ, CBL, FBZ, TBZ, NAA, CBF, DCP and MBC, respectively. PMT = 450 V.

agrochemicals were the fungicides FBZ, TBZ, DCP and MBC, the insecticides CBL and CBF, and the plant growth regulator NAA. From the normalized excitation spectra of these agrochemicals (Fig. 7A) it is clear that an important overlap exists with the BTZ excitation spectrum, while the overlap with the normalized BTZ emission spectrum is less significant. However, if the spectra are plotted using the actual concentrations of agrochemicals (see below), it is confirmed that the emission of BTZ is severely interfered (Fig. 7B). In fact, with the purpose of simulating a very unfavorable situation, the interferents were added at high relative concentrations. In order to maximize the corresponding interference effect, the agrochemicals with lower quantum yields were used at higher concentrations than those with larger quantum yields. In all cases, the interferent concentrations were larger than the maximum allowed levels in natural waters, and therefore they are representative of highly contaminated waters. Using these concentrations and under the working conditions established in Table 2, a saturation of the fluorescence signal was observed in a wide spectral region of the EEFMs for these samples. Therefore, a restricted region, where the instrumental signal could be correctly measured, was selected for data processing (see Fig. 5B). The number of responsible components, selected by following a similar procedure to that indicated above for the validation samples, was also two. Taking into account that in this restricted wavelength zone the background signal is negligible, and does not significantly contribute to the total signal, the PARAFAC components were assigned to BTZ and to a combined signal corresponding to the interferents. Apparently, PARAFAC is not able to discern between the profiles of each foreign compound, and retrieves the interference profiles as a single unexpected component. However, this fact does not preclude the obtainment of good analytical results in these type of complex samples (Fig. 6), demonstrating the high level of selectivity achieved by this method. The statistical results shown in Table 3, with adequate values for RMSEP and REP, do also support this conclusion.

The LODs obtained both in the absence and presence of interferents (3 and 5 ng mL^{-1}, respectively) are acceptable taking into account that a very simple methodology is applied to complex samples.

Based on information on the environmental behaviour of BTZ, the addendum to the Guidelines for Drinking-water Quality published in 1998 by the World Health Organization, established a health-based value of 30 ng mL^{-1} for BTZ.[23] Considering this value, the proposed method could be directly applied without the necessity of a pre-concentration step. At this point, it is important to remember the effect of the cyclodextrin in the measured signals, which allowed to obtain these LOD values. However, although the presence of the organized medium significantly increases the sensitivity of the method, its effect is not large enough to allow measuring concentrations below part per billion levels. In fact, while the proposed method is able to determine BTZ concentrations in areas with profuse agricultural activity, in those samples where the levels are very low a pre-concentration step, for example by employing a solid-phase extraction, is recommended.

A previously described fluorescent method performed in *N*, *N*-dimethylformamide rendered a comparable LOD (LOD = 3.3 ng mL^{-1}),[7] although new trends in analytical methodologies emphasize the reduction of the use of organic solvents.[24,25] On the other hand, an LOD as low as 0.4 ng mL^{-1} was reported using zeroth-order data obtained from solid-phase spectrofluorimetry.[12]

As a conclusion, the most relevant advantages of the proposed method are both the employment of aqueous solutions and the selectivity attained with the second-order calibration.

In order to evaluate the application of the present method in real samples, a recovery study by spiking natural water samples with BTZ was carried out. Fig. 5C and D show the contour plots of the EEFMs of typical real samples added with BTZ. As can be observed in these figures, the investigated natural matrices are complex, since they have background signals significantly different from that corresponding to a validation sample (shown in Fig. 5A) containing BTZ at a similar concentration. However, the fluorescence background of the matrices was not high enough to preclude the measurement in the complete wavelength range. Two or three PARAFAC factors were estimated in these real samples. Four different concentrations (including $C_{BTZ} = 0$) were analyzed in each sample, and the excellent results obtained (Fig. 6 and Table 3) suggest that the method can overcome the problem of the presence of unexpected interferents (*e.g.* polycyclic aromatic hydrocarbons, humic acids, *etc.*) from the background of the real samples.

Conclusion

BTZ emits a weak fluorescence in aqueous solution above pH 4, when it is present in its anionic structure. This signal does not seriously vary with the temperature, but is significantly enhanced in the presence of certain organized media, which shield the excited BTZ molecule from non-radiative pathways. Micellar systems formed by HTAB and HTAC produced better results than DeTAB and neutral and anionic surfactants, showing the preference of the anionic analyte for cationic surfactants with long non-polar chains. The effect of selected β-cyclodextrin derivatives on the fluorescence emission of BTZ is more significant than those produced by micellar systems. Among the studied cyclodextrins, M-β-CD led to the best enhancement, and was selected as auxiliary reagent for the quantitative analysis. Excitation–emission fluorescence matrices of BTZ in the presence of M-β-CD were processed by PARAFAC, allowing its successful determination at part per billion levels in both artificial samples with spectral interferents and real water samples. Sub-part per billion BTZ residues would require a pre-concentration step.

Acknowledgements

Authors thank the financial support of this research provided by Consejo Nacional de Investigaciones Científicas y Técnicas (Project PIP 1950) and Universidad Nacional de Rosario.[26]

References

1 K. Müller, G. N. Magesan and N. S. Bolan, *Agric., Ecosyst. Environ.*, 2007, **120**, 93–116.
2 A. M. Powe, S. Das, M. Lowry, B. El-Zahab, S. O. Fakayode, M. L. Geng, G. A. Baker, L. Wang, M. E. McCarroll, G. Patonay, M. Li, M. Aljarrah, S. Neal and I. M. Warner, *Anal. Chem.*, 2010, **82**, 4865–4894.
3 K. B. Li, J. T. Cheng, X. F. Wang, Y. Zhou and W. P. Liu, *Pedosphere*, 2008, **18**, 265–272.
4 R. Loos, G. Locoro, S. Comero, S. Contini, D. Schwesig, F. Werres, P. Balsaa, O. Gans, S. Weiss, L. Blaha, M. Bolchi and B. M. Gawlik, *Water Res.*, 2010, **44**, 4115–4126.
5 M. Bach, M. Letzel, U. Kaul, S. Forstner, G. Metzner, J. Klasmeier, S. Reichenberger and H. G. Frede, *Water Res.*, 2010, **44**, 3725–3733.
6 M. Peschka, M. Petrovic, T. P. Knepper and D. Barceló, *Anal. Bioanal. Chem.*, 2007, **388**, 1227–1234.
7 F. García Sánchez, A. Navas Díaz and R. Fernández Correa, *Anal. Chim. Acta*, 1992, **259**, 61–66.
8 T. C. Mueller, T. B. Moorman and M. A. Locke, *Weed Sci.*, 1992, **40**, 270–274.
9 R. T. Krause, *J. Chromatogr., A*, 1983, **255**, 497–510.
10 C. J. Miles and H. Anson Moye, *Anal. Chem.*, 1988, **60**, 220–226.
11 W. Schüssler, *Chromatographia*, 1990, **29**, 24–30.
12 J. L. Vilchez, D. Torres Bustos, R. Blanc and A. Navalón, *J. AOAC Int.*, 1996, **79**, 567–570.
13 C. Yañez, M. Araya and S. Bollo, *J. Inclusion Phenom. Macrocyclic Chem.*, 2010, **68**, 237–241.
14 R. Bro, *Chemom. Intell. Lab. Syst.*, 1997, **38**, 149–171.
15 A. Rinnan, J. Riu and R. J. Bro, *J. Chemom.*, 2007, **21**, 76–86.
16 G. N. Piccirilli and G. M. Escandar, *Analyst*, 2010, **135**, 1299–1308.
17 M. J. Culzoni, R. Q. Aucelio and G. M. Escandar, *Talanta*, 2010, **82**, 325–332.
18 S. G. Schulman, Acid–Base Chemistry of Excited Singlet States, in *Modern Fluorescence Spectroscopy*, ed. E. L. Wehry, Plenum Publishing Corporation, New York, 1976, vol. 2, ch. 6.
19 E. Pramauro, E. Pelizzetti, Surfactants in Analytical Chemistry. Applications of Organized Amphiphilic Media, in *Wilson & Wilson's Comprehensive Analytical Chemistry*, ed. S. G. Weber, Elsevier, Amsterdam, The Netherlands, 1996, vol. 31, ch. 4.
20 E. Sánchez and B. R. Kowalski, *Anal. Chem.*, 1986, **58**, 496–499.
21 R. Bro and H. L. A. Kiers, *J. Chemom.*, 2003, **17**, 274–286.
22 A. G. González, M. A. Herrador and A. G. Asuero, *Talanta*, 1999, **48**, 729–736.
23 *Guidelines for Drinking-Water Quality*, World Health Organization, Geneva, 3rd edn, 2004, vol. 1.
24 J. A. Linthorst, *Found. Chem.*, 2010, **12**, 55–68.
25 J. G. Ibanez, M. Hernandez Esparza, C. Doria Serrano, A. Fregoso Infante, M. M. Singh, *Environmental Chemistry. Fundamentals*, Springer, New York, 2007, ch. 12.
26 S. A. Bortolato, J. A. Arancibia and G. M. Escandar, *Anal. Chem.*, 2008, **80**, 8276–8286.

